Detection of macroalgae blooms by complex SAR imagery

Article *in* Marine Pollution Bulletin · November 2013

DOI: 10.1016/j.marpolbul.2013.10.044 · Source: PubMed

4 authors, including:

Hui Shen
Bedford Institute of Oceanography
78 PUBLICATIONS **759** CITATIONS

SEE PROFILE

W. Perrie
Bedford Institute of Oceanography, Fisheries and Oceans Canada
278 PUBLICATIONS **4,742** CITATIONS

SEE PROFILE

Yijun He
Nanjing University of Information Science & Technology
237 PUBLICATIONS **1,817** CITATIONS

SEE PROFILE

Marine Pollution Bulletin 78 (2014) 190–195

Contents lists available at ScienceDirect

Marine Pollution Bulletin

journal homepage: www.elsevier.com/locate/marpolbul

Detection of macroalgae blooms by complex SAR imagery

Hui Shen [a,b,c], William Perrie [b,*], Qingrong Liu [d], Yijun He [e]

[a] Institute of Oceanology, Chinese Academy of Sciences, 7 Nanhai Road, Qingdao 266071, China
[b] Fisheries and Oceans Canada, Bedford Institute of Oceanography, 1 Challenger Drive, Dartmouth B2Y 4A2, Canada
[c] Key Laboratory of Ocean Circulation and Waves, Chinese Academy of Sciences, 7 Nanhai Road, Qingdao 266071, China
[d] North China Sea Branch of the State Oceanic Administration, 27 Yuanling Road, Qingdao 266061, China
[e] Nanjing University of Information Science and Technology, 4 Longshanbei Road, Nanjing 210044, China

ARTICLE INFO

Keywords:
Green macroalgae blooms
Synthetic aperture radar (SAR)
High resolution early detection
Unsupervised SAR index factor

ABSTRACT

Increased frequency and enhanced damage to the marine environment and to human society caused by green macroalgae blooms demand improved high-resolution early detection methods. Conventional satellite remote sensing methods via spectra radiometers do not work in cloud-covered areas, and therefore cannot meet these demands for operational applications. We present a methodology for green macroalgae bloom detection based on RADARSAT-2 synthetic aperture radar (SAR) images. Green macroalgae patches exhibit different polarimetric characteristics compared to the open ocean surface, in both the amplitude and phase domains of SAR-measured complex radar backscatter returns. In this study, new index factors are defined which have opposite signs in green macroalgae-covered areas, compared to the open water surface. These index factors enable unsupervised detection from SAR images, providing a high-resolution new tool for detection of green macroalgae blooms, which can potentially contribute to a better understanding of the mechanisms related to outbreaks of green macroalgae blooms in coastal areas throughout the world ocean.

1. Introduction

Explosive proliferation of *ulva prolifera* leads to green macroalgae blooms, whereby massive accumulated unattached green macroalgae form into a "green tide" causing major ecological and economic impacts globally (Fletcher, 1996; Hu et al., 2010). The outbreak of these blooms is generally related to coastal eutrophication resulting from excessive nutrients and pollutants that are dumped into the ocean from agriculture, aquaculture, industries, and urbanization (Hu et al., 2010). The spatial distributions of green macroalgae blooms are often restricted to local coastal areas. However, with increasing human developments in coastal areas, the frequency of green macroalgae blooms has been accelerating by as much as 10-fold, for example, comparing the 1950s to the 2000s on the West Florida Shelf of United States (Brand and Compton, 2007). Moreover, the spatial coverage can expand to cover a vast ocean area, as with the world's largest 'green tide' which tends to occur in the Yellow Sea (YS) and East China Sea (ECS) (Hu et al., 2010).

Since the first massive YS bloom in June 2008, attracting world-wide attention because of its devastating threat to the 29th Olympic Games Sailing Event/Competition, green macroalgae have continued to dramatically develop each year, from April to July, in the coastal seas of China. Huge efforts have been put in place to try to remove the macroalgae blooms from these coastal seas in order to protect aquaculture, tourism and diminish the social effects on coastal cities.

Early detection of the outbreak of a green macroalgae bloom is vitally important for decision-making and remedial measures. Satellite remote sensing has contributed to detection of the location and spatial coverage of green macroalgae over vast ocean areas, using spectra radiometer observations from MODIS (1999-) and MERIS (2002–2012) to gather information on green macroalgae areas from space. By combination of spectral radiances (above the atmosphere) in different channels, macroalgae patches stand out from spectral radiometer images of the ocean surface. Hu (2009) developed a Floating Algae Index based on MODIS satellite data (with 859 nm wavelength) for the detection of floating algae over the ocean surface. Gower and King (2011) applied a Maximum Chlorophyll Index to MERIS data (with 709 nm wavelength) for detection of *Sargassum*. Marmorino et al. (2011) performed airborne hyperspectral and thermal infrared investigations of the *Sargassum* drift line in waters off the East Coast of Florida, USA. Cui et al. (2012) compared the ability of different satellite data to monitor green macroalgae blooms, including the charge-couple device (CCD) data, SAR data, and spectra radiometer data. The

* Corresponding author. Tel.: +1 902 4263985.
E-mail addresses: shenhui@qdio.ac.cn (H. Shen), william.perrie@dfo-mpo.gc.ca (W. Perrie), liuqingrong@nmfc.gov.cn (Q. Liu), yjhe@nuist.edu.cn (Y. He).

0025-326X/$ - see front matter Crown Copyright © 2013 Published by Elsevier Ltd. All rights reserved.
http://dx.doi.org/10.1016/j.marpolbul.2013.10.044

ability of spectra radiometer data, through various index factors, to identify green macroalgae apart from other signals in satellite imagery, makes it unique for monitoring of macroalgae blooms from space.

However, spectra radiometers can monitor the ocean surface only when the sky is cloud-free. Clouds blind the spectra radiometer to ocean surface phenomena, making it impossible to observe green macroalgae, which also limits the calculation of statistics required for related studies. This is a problem for detection of the 'world's largest green tides' in the YS and ECS, because they often coincide with the rainy season and MODIS spectra radiometer images are limited by the associated vast cloud coverage. Moreover, although many studies claim that the massive green macroalgae outbreaks are caused by enhanced aquaculture off the east coast of China (Pang et al., 2010), thus far, the closest evidence of this from remote sensing are the macroalgae patches which are found 40 km from the coast in MODIS imagery. Hu et al. (2010) suggest that the coarse resolution of the MODIS imagery ($\geqslant$250 m) limits the early detection of green macroalgae, before they expand into large blooms.

Synthetic aperture radar (SAR) has much higher spatial resolution (up to 3 m for fine mode RADARSAT-2 SAR) and can penetrate cloud and monitor the ocean surface in almost all weather conditions. SAR is also superior to MODIS for nearshore and coastal ocean monitoring and for retrieval of oceanic parameters such as marine winds in severe weather conditions. Thus far, limited research has been performed on the capability of SAR to detect green macroalgae. Although SAR's potential for all weather monitoring of green macroalgae has been recognized (Jiang et al., 2009), methods to detect green macroalgae from SAR images greatly depend on our ability to visually distinguish green macroalgae's backscattered signals from those of other targets, such as ships, islands, and other ocean processes, including winds, currents, fronts, and marine slicks. Until now, efforts to set up a threshold value for automatic recognition of green macroalgae from SAR images have not been successful.

Many studies have shown that application of combinations of different polarization measurements of SAR can contribute to better interpretation of the data. Kudryavtsev et al. (2013) illustrated a capability to recognize different ocean surface features, such as ocean currents, slicks, wind, by combining co-polarized SAR (VV and HH) data into polarization differences, polarization ratios and nonpolarized components. Our objective is to establish a capability for unsupervised recognition of green macroalgae based on fully polarized RADARSAT-2 quad-pol SAR imagery. In Section 2, we introduce the data used for this study. The polarimetric characteristics of green macroalgae are presented in Section 3. A new SAR-derived variable for unsupervised recognition of green macroalgae from quad-pol SAR images is introduced in Section 4. Discussions and conclusions are given in Section 5.

2. Data

We collected RADARSAT-2 SAR images of an area covered by the vast green macroalgae blooms occurring in the Yellow Sea and South China Sea from June 1 to July 31 in 2012. Besides wide swath SCANSAR mode images, we also used fine mode quad-pol SAR images with 25 km $\times$ 25 km coverage in 4 polarizations (HH, VH, HV, VV).

Results presented in this study are based on two quad-pol images which are captured at 10:00 am on July 11, 2012 and 09:56 am July 24, 2011, with spatial resolution of 4.7 m in the radar range direction and 4.8 m in the azimuth. The spatial coverage of the image is the northern part of Yellow Sea, with the coastal region including an area that has suffered invasion by green macroalgae (Figs. 1 and 4).

3. Polarimetric characteristics of green macroalgae

Fig. 1 shows the amplitude of the normalized backscattered radar signals of the four full polarizations. Co-polarized images (HH and VV), denoted co-pol, show stronger radar returns over the open water area, than cross polarization (cross-pol) images (HV and VH). All images exhibit clear bright slicks which are related to the green macroalgae patches on the ocean surface. The MODIS image on July 10, 2012 confirms the existence of green macroalgae in this area (Fig. 2). However, macroalgae observations cannot be obtained from MODIS imagery on July 11, 2012 due to cloud contamination (not shown). By comparison, although backscattered signals from the green macroalgae are weaker in the cross-pol images than in the co-pol SAR images, they are more clearly evident due to the strong contrast against the associated background radar returns in the cross-pol images.

For cross-polarization SAR measurements, volume scattering is the dominant mechanism, whereas for co-pol measurements, Bragg scattering is more important. Ocean processes can modulate capillary gravity waves on the ocean surface and therefore can be monitored by co-pol SAR, whereas such modulations have no apparent impact on volume scattering unless the waves break. Therefore, in the amplitude field of SAR returns, cross polarization measurements give clean patterns of the green macroalgae, with low signal strength due to the low signal to noise ratio. Although co-pol measurements have strong radar returns from the green macroalgae, other competing signals from atmospheric and oceanic dynamics may also occur, which can mask or confuse the green macroalgae signal (Jiang et al., 2009).

In addition to amplitude information, fine quad-pol RADARSAT-2 data also capture phase information for the backscattered radar signals. It has been demonstrated that the phase difference between different radar measurement times, or different radar orbits, can reveal important information about the target (Boerner et al., 1992). Here, we show the phase difference data between different polarization measurements. Fig. 1e and f gives cross-pol ($\theta_{VH} - \theta_{HV}$) and co-pol ($\theta_{HH} - \theta_{VV}$) phase differences, respectively.

The phase difference data give similar patterns that result from the amplitude fields, shown in Fig. 1a–d. In Fig. 1e, pixels observing green macroalgae have the same phase in VH and HV polarizations; however, the phase difference with respect to the open ocean water area is within the range $[\pi/2 \sim 3\pi/2]$. Similarly, in Fig. 1f, zero phase difference comes from the green macroalgae-covered areas and also from areas that have strong radar returns in the amplitude field of the co-pol field. The phase differences between cross polarization (VH or HV) and co-pol (HH or VV) were also calculated, but no obvious patterns are evident.

Comparing full polarization SAR radar returns, both amplitude and phase fields show clear patterns related to the green macroalgae covered areas. Therefore, a combination of the information from both fields has potential value for improved detection of green macroalgae on the ocean surface – using SAR imagery.

4. Index factor for green macroalgae detection from quad-pol SAR images

In radar polarimetry, a complex scattering matrix (1) is often defined to represent radar returns,

$$S = \begin{bmatrix} S_{HH} & S_{HV} \\ S_{VH} & S_{VV} \end{bmatrix} \quad (1)$$

where S is the complex scattering matrix, and S_{HH} (S_{HV}, S_{VH}, S_{VV})) represents the complex radar returns for HH (HV, VH, VV) polarization.

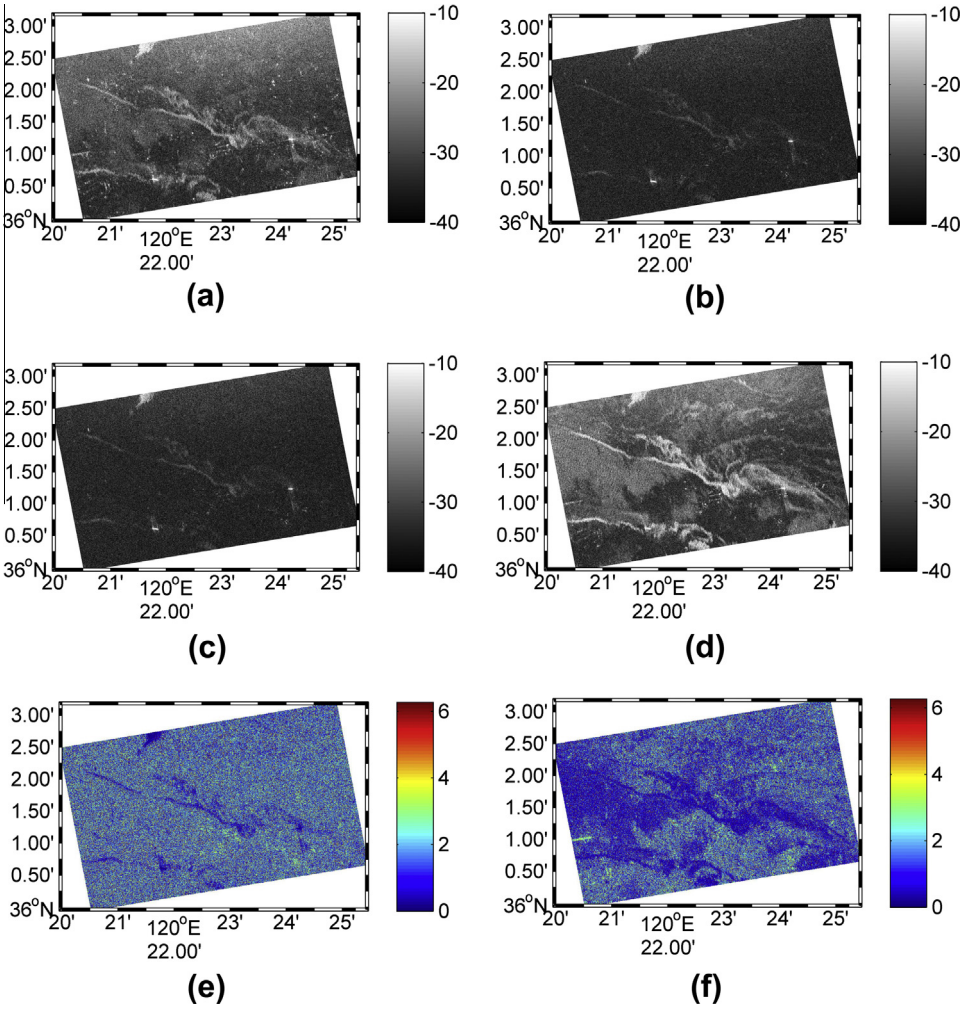

Fig. 1. A subset images of RADARSAT-2 quad-pol SAR captured in July 11, 2012 10:00:14 UTC, with amplitude field (unit: dB) for: (a) HH, (b) HV, (c) VH, (d) VV polarization; (e) and (f) for phase difference of $\theta_{VH} - \theta_{HV}$ and $\theta_{HH} - \theta_{VV}$ respectively (unit: radian). RADARSAT-2 Data and Product© MacDonald, Dettwiler and Associates Ltd., – All Rights Reserved.

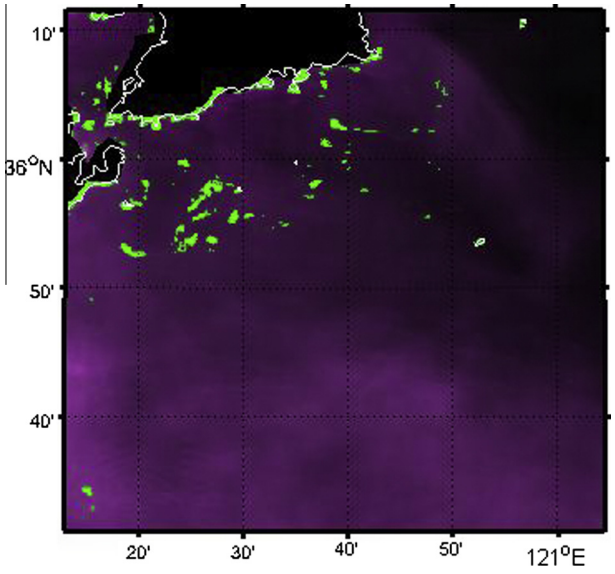

Fig. 2. A MODIS spectraradiometric false color image confirms the existence of green tide in the studied area at 03:15 July 12, 2012 UTC.

Each pixel in the full polarization image corresponds to a single scattering matrix. The coherence or covariance matrices are often applied for target decomposition purposes, such as the well-known entropy-alpha classification method (Praks et al., 2009). Based on the polarimetric characteristics presented in Section 3, we define the following index factor for co-pol SAR measurements,

$$IF_{co} = \mathrm{Re}\left(\frac{(S_{HH} - S_{VV})}{S_{VV}}\right) \tag{2}$$

where IF_{co} is the index factor for co-pol images, and "Re" stands for the real part of the complex number.

In Eq. (2), the numerator $S_{HH} - S_{VV}$ represents the backscattered strength of the target, especially from double bound scattering (Touzi et al., 2004), thereby providing a measure of the amplitude strength of the green macroalgae. The denominator S_{VV} is the radar return for the VV polarization in the complex scattering matrix in Eq. (1). As presented in Section 3, the phase of S_{VV} is the same as that of S_{HH} for green macroalgae, but opposite that of open ocean water. Therefore, the ratio of the numerator and denominator in Eq. (2) represents the phase difference between S_{VV} and S_{HH}, so that the index factor in Eq. (2) embraces contributions of both amplitude and phase differences between HH and VV radar backscatter returns.

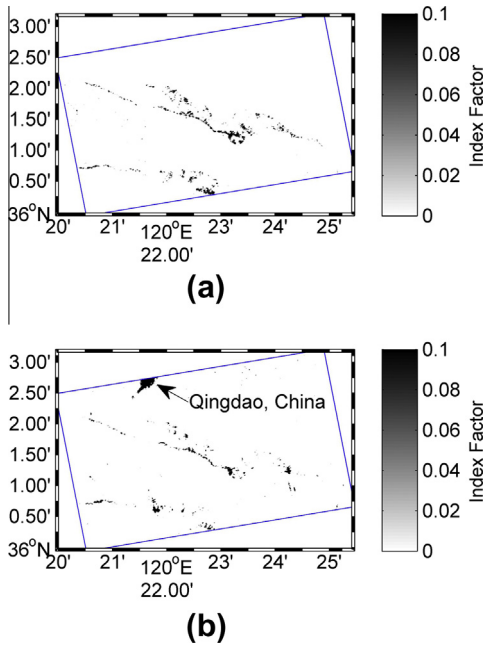

Fig. 3. Coverage of green macroalgae bloom patches detected by index factor defined in Eq. (3) from: (a) co-pol SAR image; (b) from cross-pol SAR image.

Furthermore, for co-pol radar returns, HH is generally lower than VV polarization, as can be seen in Fig. 1a and d, and the amplitude of S_{VV} is less than zero, which in this case is about [−40 dB, −10 dB]. Therefore, we have $IF_{co} > 0$ for the green macroalgae covered area, and $IF_{co} < 0$ for the open water area. The sign difference of IF_{co} between green macroalgae areas and open water, makes this index factor a possible candidate for unsupervised automatic green macroalgae detection.

Alternately, a similar index factor for cross polarization measurements is also defined, so that cross-pol mode SAR images can also be applied for macroalgae detection:

$$IF_{cross} = \mathrm{Re}\left(\frac{(2S_{HV} - S_{VH})}{S_{VH}}\right) \tag{3}$$

where IF_{cross} is the index factor for cross-pol SAR measurements. In Eq. (3), the index factor for green macroalgae detection from cross-pol SAR images has a form similar to Eq. (2) for co-pol SAR images, except that S_{HV} is multiplied by 2; this ensures that the sign of the numerator is positive, since the amplitudes of S_{HV} and S_{VH} are almost the same, according to the reciprocity theory (Boerner et al., 1992). Therefore, Eq. (3) is adopted for cross-polarization imagery, because it gives opposite signs between the green macroalgae-covered areas and the open water areas.

Fig. 3a and b gives the results of unsupervised green macroalgae detection for the image in Fig. 1, using the index factors defined by Eqs. (2) and (3) for co-pol and cross-pol SAR images, respectively. Spatial coverage of green macroalgae is clearly demonstrated by both index factors. However, in results from the cross-pol SAR image (Fig. 3b), the island located to the north of the sub-image corresponds to an index factor that is positive, and this signature cannot be removed with our unsupervised procedure. Thus, a high resolution shore line database is required so that signal contamination from land shorelines, or small islands, can be masked automatically. As the island does not appear in the co-pol image, the latter has greater potential for unsupervised detection, in this regard. However, we also present the cross-pol index factor as a tool for situations where only cross-pol data are available.

Furthermore, by counting pixels in the co-pol image in Fig. 3a, we obtain an estimate of the total amount of the green macroalgae on the ocean surface. Of the 22.95 km^2 total spatial coverage that is observed by the SAR image, 0.36 km^2 is automatically detected to be covered by green macroalgae from the co-pol data (Fig. 3a),

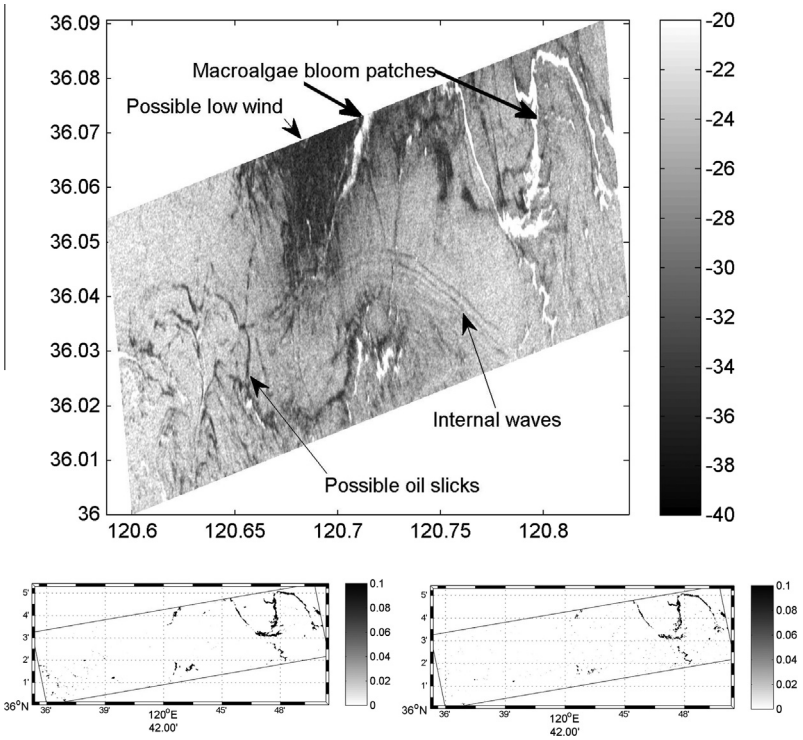

Fig. 4. Subset images from the VV mode RADARSAT-2 quad-pol SAR captured on July 24, 2011 09:56:01 UTC: (a) interpretation of image features, (b) retrieved macroalgae bloom patches, based on co-pol (left) and cross-pol index factors, as proposed in this paper. RADARSAT-2 Data and Product© MacDonald, Dettwiler and Associates Ltd., – All Rights Reserved.

and 0.20 km^2 from the cross-pol data (Fig. 3b). Assuming a conservative density of algae 1.0 k_g/m^2 (Hu et al., 2010), this suggests a total of 360 tons, and 200 tons of algae, respectively, are detected for this area from the co-pol and cross-pol mode SAR images. Additional discussion of these differing results appears in Section 5.

A second RADARSAT-2 SAR image, which was captured on July 24, 2013, is analyzed, in Fig. 4. This exhibits an internal wave pattern and additional unknown dark band features, which may be related to low winds and oil slicks, together with macroalgae patches, co-existing together in the same image. By adopting index factors proposed in Eqs. (2) and (3), patches of macroalage blooms are obtained in Fig. 4(b), which show the validity of proposed index factors for detection, in the presence of internal waves and competing ocean surface features.

5. Discussion and Conclusions

Green macroalgae blooms exert ecological, economical and social burdens for coastal areas. Limited observations in temporal and spatial domains hinder the development of a comprehensive understanding of the mechanisms controlling these macroalgae outbreaks. Satellite remote sensing can monitor green macroalgae patches floating on the ocean surface. Presently, the spectral radiometer has been generally applied to monitor green macroalgae blooms from the air and from space (Hu et al., 2010; Gower and King, 2011; Marmorino et al., 2011), but only under cloud free conditions. However, mid latitude areas, such as the Yellow Sea and East China Sea are often covered by cloud.

SAR's capability to monitor targets on the ocean surface as well as meteorological and oceanographic dynamics is widely accepted. However, most studies and applications are based on the amplitude information of radar returns, where the target can be classified by setting threshold values for different classification parameters. Due to the characteristics of individual SAR images, the threshold values often need to be tuned for satisfactory classification results. A fixed set of criteria needs to be established for unsupervised classifications. With more advanced SAR instrumentation, it has been possible to capture more detailed information about the target, such as multi-polarization characteristics. Studies have shown improved ability to interpret ocean processes from SAR by combining radar backscattered signals from different polarizations (Kudryavtsev et al., 2013).

Here, two newly defined index factors based on high resolution (4.7 m) SAR images are shown to have opposite signs for green macroalgae detection, as compared to the surrounding open water surface, and are therefore candidates for unsupervised detection of green macroalgae. Because of the high resolution of SAR images, this approach can potentially be useful to detect the precursors to green macroalgae blooms, such as occur in the Yellow Sea and the East China Sea, and other ocean areas.

Comparing the two proposed index factors for co-pol and cross-pol SAR images, co-pol has a better signal to noise ratio than cross-pol and also has the ability to distinguish land from the macroalgae-covered ocean surface. Moreover, although the Bragg scattering mechanism in co-pol SAR images also results in strong signals from other competing dynamical processes, such influences do not show up in our proposed co-pol index factor. By comparison, the volume scattering mechanisms in cross-pol SAR images have the result that the competing signals from other processes are not as obvious, as in co-pol SAR images, except for very strong phenomena such as hurricanes (Zhang and Perrie, 2012). Although RADARSAT-2 quad-pol SAR has a well-calibrated accuracy to −45 dB (Luscombe, 2008), our results suggest that additional high radiometric calibration accuracy would contribute to improved detection of green macroalgae by cross-pol SAR imagery.

The signal-to-noise ratios for the co-pol and cross-pol SAR images are different because of different target detection mechanisms, respectively, leading to different results for detected macroalgae (in Fig. 3). Thus, cross-pol data suggest less macroalgae than co-pol data. Moreover, in addition to a better signal-to-noise ratio, co-pol imagery can also detect the presence of macroalgae beneath the water surface due to its influence on Bragg scattering, which will not be detected in cross-pol data where volume scattering mechanisms are dominant. However, the general location and overall coverage of the macroalgae area is detected by both SAR modes. Therefore, the proposed index factors for both modes are important in detecting the macroalgae area, although co-pol data clearly has better detection ability.

Our proposed index can be directly applied to RADARSAT-2 quad-pol SAR images which provide 4 full polarization images simultaneously; however the domain of their spatial coverage is small (25 km × 25 km) and thus not practical for operational monitoring of large areas. By comparison, although RADARSAT-2 dual-pol ScanSAR measurements have wider coverage (500 km × 500 km), operating in HH + HV or VH + VV mode, they cannot be used because our proposed index factors require two co-pol or two cross-pol images at the same time. We suggest that future missions include dual-pol mode images with co-pol and cross-pol polarizations for detection of green macroalgae over large spatial areas, as was possible for Envisat ASAR imagery.

Unlike the spectral radiometer, which can capture ocean color changes to depths of 10 m beneath the water surface (Marmorino et al., 2011), SAR can only observe the ocean surface. Therefore, the proposed index factors are only applicable to detect macroalgae bloom patches that reach the ocean surface, which show up as bright bands in SAR images due to enhanced strong backscatter. However, macroalgae patches that are beneath the water surface tend to exhibit dark bands in SAR images, due to suppressed Bragg waves; this was suggested by Gower and King (2011) from their investigations of *Sargassum*, a kind of brown algae. Additional studies are required to discover the influence of such differences on algae detection methods for SAR.

In conclusion, we have given the polarimetric characteristics of green macroalgae blooms, compared to open water areas, in both amplitude and phase domains, based on quad-pol RADARSAT-2 SAR images. New index factors have been defined which show opposite signs in green macroalgae covered areas, compared to open water areas. These index factors enable unsupervised detection of green macroalgae blooms from co-pol (HH and VV) or cross-pol (VH and HV) SAR images. We believe this study provides potential new tools to detect green macroalgae blooms and thus, together with spectral radiometer data and available *in situ* measurements, fosters better understanding of the processes leading to the outbreak of blooms in coastal areas.

Acknowledgements

The authors thank the reviewers and the Editor for detailed comments and suggestions. RADARSAT-2 images are kindly provided by the Canadian Space Agency (CSA). This work is supported by National Science Foundation of China (No. 40906091), State High-Tech Development Plan of China (2013AA09A505) and Canadian "Spaceborne Ocean Intelligence Network (SOIN)" project, and the Panel on Energy Research and Development (PERD).

References

Boerner, W.-M., Yan, W., Xi, A., Yamaguchi, Y., 1992. Basic concepts of radar polarimetry. In: Boerner, W.-M. et al. (Eds.), Proceedings of the NATO Advances Research Workshop on ' Direct and Inverse Methods in Radar Polarimetry', Bad Windsheim, Germany, September 18–24, 1988, vol. 350 (part 1). Kluwer Academic Publishers, Dordrecht, pp. 155–245.

Brand, L., Compton, A., 2007. Long-term increase in Karenia brevis abundance along the southwest Florida Coast. Harmful Algae 6, 232–252. http://dx.doi.org/10.1016/j.hal.2006.08.005.

Cui, T., Zhang, J., Sun, L., Jia, Y., Zhao, W., Wang, Z., Meng, J., 2012. Satellite monitoring of massive green macroalgae bloom (GMB): imaging ability comparison of multi-source data and drifting velocity estimation. International Journal of Remote Sensing 33 (17), 5513–5527.

Fletcher, R.L., 1996. The occurrence of 'green tides': a review. In: Schramm, W., Nienhuis, P.H. (Eds.), Marine Benthic Vegetation: Recent Changes and the Effects of Eutrophication. Springer, Berlin, pp. 7–43.

Gower, J.F.R., King, S.A., 2011. Distribution of floating *Sargassum* in the Gulf of Mexico and the Atlantic Ocean mapped using MERIS. International Journal of Remote Sensing 32 (7), 1917–1929. http://dx.doi.org/10.1080/01431161003639660.

Hu, C., 2009. A novel ocean color index to detect floating algae in the global oceans. Remote Sensors Environment 113, 2118–2129. http://dx.doi.org/10.1016/j.rse.2009.05.012.

Hu, C., Li, D., Chen, C., Ge, J., Muller-Karger, F.E., Liu, J., Yu, F., He, M.-X., 2010. On the recurrent *Ulva prolifera* blooms in the Yellow Sea and East China Sea. Journal Geophysics Research 115, C05017. http://dx.doi.org/10.1029/2009JC005561.

Jiang, X., Zou, Y., Wang, H., Zhu, H., 2009. Application study on quick extraction of Entermorpha prolif era information using SAR data. Acta Oceanologica Sinica 31 (2), 63–68.

Kudryavtsev, V., Chapron, B., Myasoedov, A., Collard, F., Johannessen, J., 2013. On dual co-polarized SAR measurements of the Ocean surface, IEEE Geosci. Remote Sensing Letter 10 (4). http://dx.doi.org/10.1109/LGRS.2012.2222341.

Luscombe, A., 2008. RADARSAT-2 polarimetric mode calibration and data quality assessment. In: Proc. CEOS SAR Calibration and Validation Workshop, Oberpfaffenhofen, Germany, 27–28 November, 2008.

Marmorino, G.O., Miller, W.D., Smith, G.B., Bowles, J.H., 2011. Airborne imagery of a disintegrating Sargassum drift line. Deep Sea Research Part I 58 (3), 316–321.

Pang, S.J., Liu, F., Shan, T., Xu, N., Zhang, Z., Gao, S., Chopin, T., Sun, S., 2010. Tracking the algal origin of the Ulva bloom in the Yellow Sea by a combination of molecular, morphological and physiological analyses. Marine Environmental Research 69 (4), 207–215. http://dx.doi.org/10.1016/j.marenvres.2009.10.007.

Praks, J., Koeniguer, E.C., Hallikainen, M.T., 2009. Alternatives to target entropy and alpha angle in SAR polarimetry. IEEE Transactions on Geoscience and Remote Sensing 47 (7), 2262–2274.

Touzi, R., Boerner, W.M., Lee, J.S., Lueneburg, E., 2004. A review of polarimetry in the context of synthetic aperture radar: concepts and information extraction. Canadian Journal of Remote Sensing 30 (3), 380–407. http://dx.doi.org/10.5589/m04-013.

Zhang, B., Perrie, W., 2012. Cross-polarized synthetic aperture radar: a new potential measurement technique for hurricanes. Bulletin of the American Meteorological Society, 531–541. http://dx.doi.org/10.1175/BAMS-D-11-00001.1.